Bull. Mater. Sci., Vol. 39, No. 1, February 2016, pp. 229–234. © Indian Academy of Sciences.

Radical coupling of maleic anhydride onto graphite to fabricate oxidized graphene nanolayers

FATEMEH SAMADAEI[1,2], MEHDI SALAMI-KALAJAHI[1,2,*] and HOSSEIN ROGHANI-MAMAQANI[1,2]

[1]Department of Polymer Engineering, Sahand University of Technology, P.O. Box 51335-1996, Tabriz, Iran
[2]Institute of Polymeric Materials, Sahand University of Technology, P.O. Box 51335-1996, Tabriz, Iran

MS received 17 July 2015; accepted 28 September 2015

Abstract. **Radical coupling was used to modify graphite with maleic anhydride (MAH). Azobisisobutyronitrile (AIBN) as radical generator activated MAH radically and it was reacted with defects at the surface of nanolayers. A set of batches with different reaction times (24, 48 and 72 h) were performed to obtain fully-modified nanolayers (GMA1, GMA2 and GMA3, respectively). Fourier transform infrared results approved the synthesis of MAH-grafted graphite. Thermogravimetric analysis showed that 5.9, 11.1 and 13.2 wt% of MAH was grafted onto the surface of GMA1, GMA2 and GMA3, respectively, and that was approved by X-ray photoelectron spectroscopy results. Also, X-ray diffraction patterns showed that *d*-spacing increased from 0.34 nm for graphite to 1.00 nm for all modified samples. However, GMA1 showed a weak peak related to graphite structure that disappeared when reaction time was increased. After modification with MAH, lamella flake structure of graphite was retained whereas the edges of sheets became distinguishable as depicted by scanning electron microscopy images. According to Raman spectra, modification progression resulted in more disorder structure of nanolayers due to grafting of MAH. Also, transmission electron microscopy images showed graphite as transparent layers while after modification, surface of nanolayers became folded due to the opposite effects of π-conjugated domains and electrostatic repulsion of oxygen-containing groups.**

Keywords. **Graphene oxide; chemical synthesis; maleic anhydride; XPS; Raman spectroscopy.**

1. Introduction

Graphene as one-atom-thick planar nanosheet has obtained much attention owing to its remarkable properties such as superior mechanical [1] and excellent electronic transport properties [2]. In the most applications, graphene should be modified to overcome its agglomeration and reach better dispersion [3,4]. The most useful method to produce modified-graphene is oxidation of graphite to graphene oxide (GO) and subsequently modification of GO with modifiers [5,6]. However, oxidation process is performed under harsh conditions with different oxidizing agents such as strong acids and their salts, hydrogen peroxide and potassium permanganate [3–6]. Thus, radical coupling of functional-groups-containing molecules to the surface of nanolayers may be an appropriate alternative functionalization method as previously performed about multiwalled carbon nanotube (MWCNT) [7]. In this field, maleic anhydride (MAH) is widely grafted onto different polymer chains [8–10]. Conclusively, MAH can be used in radical coupling and reaction with graphite. In this work, radical coupling of MAH onto graphite has been conducted with azobisisobutyronitrile (AIBN) as radical generator with different modification times. Fourier transform infrared (FT-IR) spectroscopy and Raman spectroscopy were used to characterize different bands in the products. Amounts of grafted MAH were obtained by thermal gravimetric analyses (TGA) and X-ray photoelectron spectroscopy (XPS) and structural properties were investigated by X-ray diffraction (XRD), scanning electron microscopy (SEM) and transmission electron microscopy (TEM).

2. Experimental

2.1 *Materials*

MAH (Merck, ≥99%), graphite fine powder (Merck, extra pure), AIBN (Acros, 99%) and methanol (Merck, 99.9%) were used as received.

2.2 *Synthesis of MAH-modified graphite*

Methanol was used as efficient solvent of MAH [11]. Metha nol do not react with MAH except under specific conditions in catalytic systems [12]. Radical coupling was used to modify graphite with MAH. Briefly, MAH (2.0 g) and graphite (1.0 g) were dispersed in methanol (100 ml) by ultrasonication (30 min) in room temperature. Then, AIBN (1.6 g) was added into the mixture and temperature was raised to boiling point of methanol. Reaction was continued under nitrogen atmosphere for 24, 48 and 72 h for GMA1, GMA2

*Author for correspondence (m.salami@sut.ac.ir)

Scheme 1. Radical coupling of MAH onto graphite to produce MAH-grafted nanolayers.

and GMA3, respectively. Modified flakes were obtained via centrifugation (1000 rpm) and washing with methanol several times. After filtration, obtained powders were dried by vacuum at 50°C. Scheme 1 shows the reaction mechanism and structure of modified nanolayers.

2.3 *Instrumentation*

FT-IR spectroscopy were performed by means of a Bruker Tensor 27 FT-IR-spectrophotometer, in the range between 500 and 4000 cm^{-1} with a resolution of 4 cm^{-1}. An average of 24 scans has been carried out for each sample. The samples were prepared on a KBr pellet in vacuum desiccators under a pressure of 0.01 Torr. TGA were carried out by means of a PL thermo-gravimetric analyzer (Polymer Laboratories, TGA 1000, UK). All samples (about 10 mg) were heated from ambient temperature to 600°C at a heating rate of 10°C min^{-1} and nitrogen as the purging gas was used at a flow rate of 50 ml min^{-1}. XRD spectra were performed on an XRD instrument (Siemens D5000) with a Cu target ($\lambda = 0.1540$ nm) at room temperature. The system consists of a rotating anode generator which operated at 35 kV and 20 mA. The samples were scanned from $2\theta = 2$–30° at the step scan mode. The diffraction pattern was collected using a scintillation counter detector. Raman spectroscopy were performed in the range from 1000 to 3000 cm^{-1} using Bruker Dispersive Raman Spectrometer fitted with a 785 nm laser source, a CCD detector and a confocal depth resolution of 2 μm. The laser beam was focused on the sample using an optical microscope. A Vega Tescan SEM analyser (Czech Republic) was used to evaluate the morphology of samples which were gold coated using a sputtering coater. The specimens were prepared by coating a thin layer on a mica surface using a spincoater (Modern Technology Development Institute, Iran). TEM, Tescan Mira, with an accelerating voltage of 120 kV was used to study the morphology of samples. All the samples were prepared by a drop-dry method on carbon-coated copper grids. X-ray photoelectron spectroscopy (XPS) was carried out using a Gamma data-Scienta Esca 200 hemispherical analyzer equipped with an AlKα (1486.6 eV) X-ray source.

3. Results and discussion

The synthesis of MAH-grafted nanosheets was monitored by means of FT-IR as depicted in figure 1 (spectra for graphite and GMA1). In graphite spectrum, the strong characteristic peak at 3430 cm^{-1} is related to the water molecules absorbed by sample or KBr powder [13]. The stretching vibrations of aromatic C=C bonds are observed at 1640 and 1575 cm^{-1} [14]. After reaction with MAH, the asymmetric and symmetric stretching of C=O band of MAH appears at 1850 and 1775 cm^{-1}, respectively [15,16]. Also, peaks at 1250 and 1030 cm^{-1} are attributed to the asymmetric and symmetric ring stretching (=C–O–C=) of cyclic ethers [16]. The appearance of the ring stretching vibration of saturated cyclic five-membered anhydride at 915 cm^{-1} instead of two sharp bands at 867 and 892 cm^{-1} due to the C=C stretching of

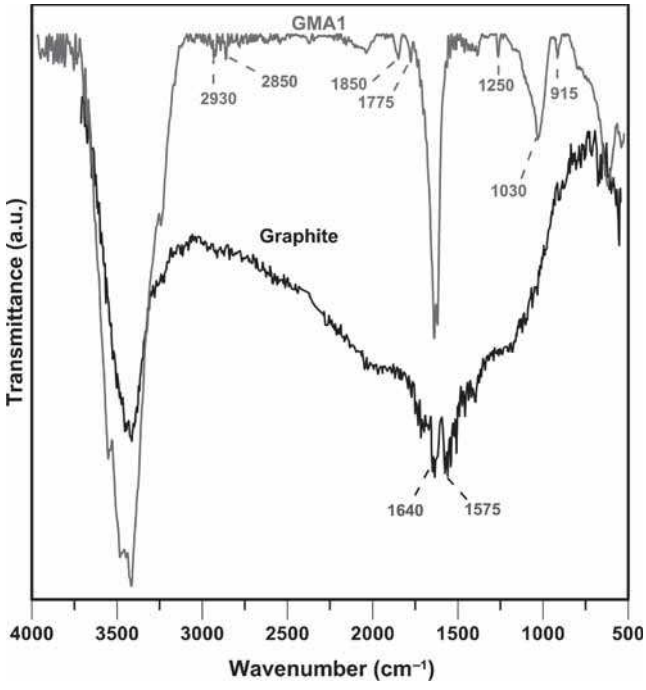

Figure 1. FT-IR spectra of graphite and GMA1.

monomeric MAH [17] further confirms that MAH is grafted onto nanolayers. The peaks at 2850 and 2930 cm^{-1} are also assigned to the stretching vibration of C–H bonds introduced by MAH molecules [18,19].

XPS was used to obtain the chemical composition of samples (figures 2 and 3). Figure 2 shows the survey data of graphite, GMA1, GMA2 and GMA3. Also, the higher resolution data of O 1s and C 1s of GMA1 are depicted in figure 3. Graphite shows an asymmetric C 1s peak centred at 284.5 eV. Also, surface oxygen content of graphite is 1.77% which correlates with 1.5–2.0% reported in literature [20]. This minor O component exists in the form of C–OH and C–O–C groups [21]. Survey-scan spectra of GMA1, GMA2 and GMA3 vary compared with graphite whereas oxygen content increases to 6.88, 13.06 and 14.73%, respectively. This shows that oxygen content increases with modification progression whereas a little increment can be seen from GMA2 to GMA3. Because of the fact that XPS measures the atomic percentage and because of the structure of MAH that contains 4 carbon and 3 oxygen atoms, oxygen contents are not much high with respect to GO prepared by acidic oxidation as reported previously [22]. C 1s band spectrum in binding energy between 280 and 290 eV and O 1s between 528 and 536 eV are used to evaluate the proportion of various functional groups in GMA1 [23]. The C 1s spectrum shows a 3.2% oxygen-containing carbon in the form of C(O)O and a 3.2% in the form of C–C(O)O both related to grafted MAH molecules. However, the signal at a binding energy of 284.6 eV shows the retained graphitic carbon structure in which aromatic sp^2 carbon atoms are present [24]. Also, C–O–C presents a 2.0 at% content related to graphite structure. O 1s higher resolution data prove that MAH structure is grafted onto nanolayers and atomic ratio of carbonyl oxygen per anhydride oxygen is approximately 2.

For further proving the success of modification process, samples were analysed by means of TGA as depicted in figure 4. According to the results, graphite shows no significant weight loss up to 600°C. However, modified samples show two weight loss stages; the first stage around 100°C is ascribed to the loss of moisture and adsorbed water molecules in π-stacked structure of MAH-functionalized nanolayers [25]. A major weight loss between 130 and 600°C for all modified samples is assigned to degradation of grafted MAH molecules [26] and corresponds to the weight loss of 5.9, 11.1 and 13.2 wt% for GMA1, GMA2 and GMA3, respectively. Due to existence of oxygen-containing moieties in the structure of MAH, MAH-modified samples show a relatively low thermal stability. Also, results show no significant difference of weight loss between GMA2 and GMA3 that is attributed to the reaction of MAH with limited scavenger centres at the surface of nanolayers [27].

XRD patterns of graphite, GMA1, GMA2 and GMA3 are shown in figure 5. Graphite shows a basal reflection (002) peak at $2\theta = 26.0°$ (d-spacing = 0.34 nm) [28]. After modification of graphite with MAH, the 002 reflection peak is

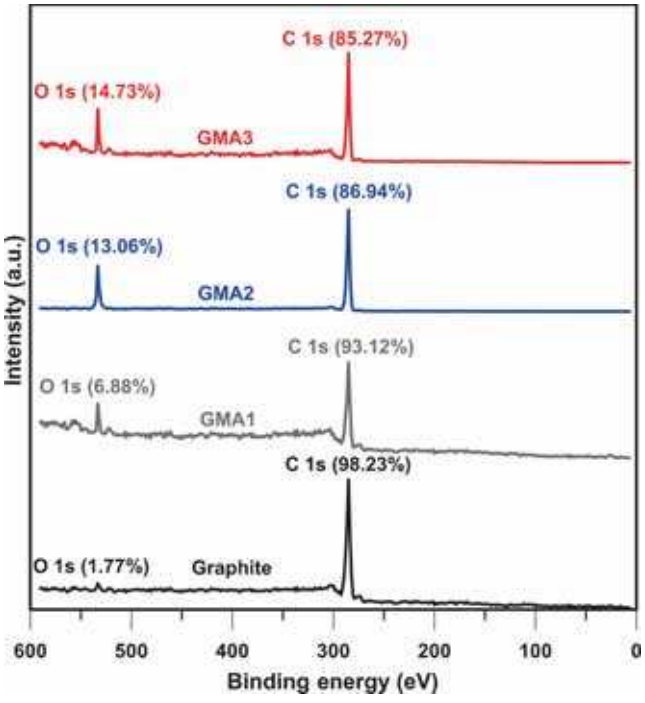

Figure 2. Wide-scan XPS spectra of graphite, GMA1, GMA2 and GMA3.

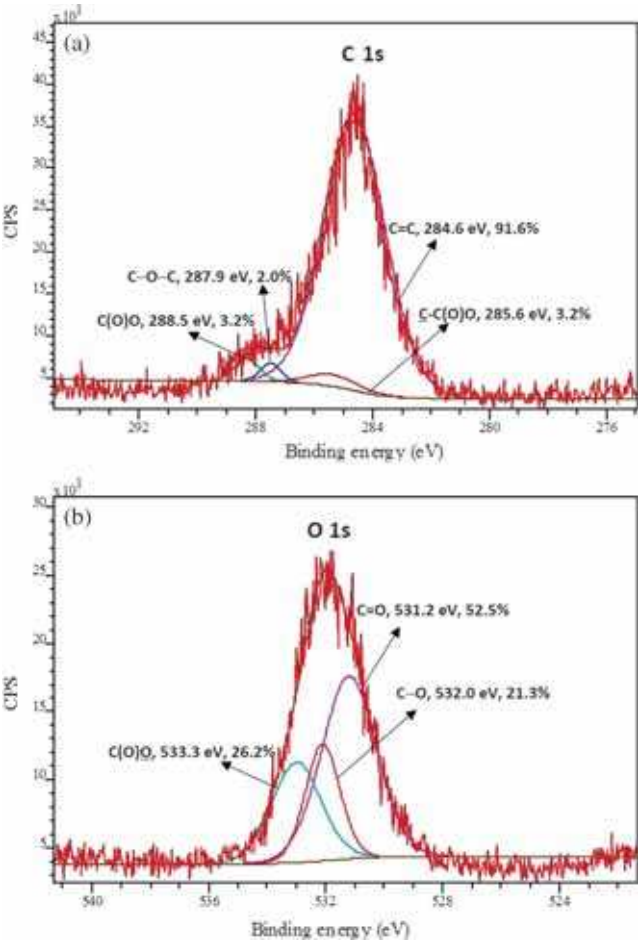

Figure 3. (**a**) C 1s and (**b**) O 1s core-level spectra for GMA1.

shifted to lower angle at $2\theta = 8.8°$ (d-spacing = 1.00 nm), revealing that d-spacing increases due to the intercalation effect of MAH in between the basal plane of graphite. However, GMA1 shows another sharp peak at $2\theta = 26.0°$ with lower intensity with respect to graphite. This shows that there are some graphitic structures that are not modified via radical coupling whereas modified flakes shows higher d-spacing value. To visually prove such a phenomenon, the morphology of graphite and GMA1 were analysed by SEM as depicted in figure 6. Graphite shows a lamella flake structure with indiscernible graphene layers. After modification with MAH, lamella flake structure is retained whereas the edges of sheets become distinguishable. However, a little graphitic structure in some regions leads to a small peak at $2\theta = 26.0°$ as discussed in XRD results. As depicted in figure 5, peak related to graphite structure disappears when coupling time increases up to 48 and 72 h. This is assigned to completely reaction of MAH molecules with surface of nanolayers. However, basal reflection peak remains unchanged at $2\theta = 8.8°$. This is attributed to the small size of MAH molecules which is not able to more intercalation of nanolayers [29]. Also, according to SEM image of GMA2 (figure 6), homogeneous dispersion of GMA2 nanolayers is achieved whereas no distinct graphite structure can be observed.

Ordered and disordered structures of carbon in graphite, GMA1, GMA2 and GMA3 were studied by Raman spectroscopy (figure 7). Graphite spectrum shows three characteristic peaks around 1312 cm^{-1} (disorder or D-mode), 1577 cm^{-1} (tangential G-mode) and 2638 cm^{-1} (2D or G′ band). D-mode is ascribed to the defects in graphene layers and the edge effect of graphene crystallites. Thus, a perfect graphite crystal should not exhibit the D band. However, for most commercial graphite products, high-temperature treatments during production introduce some defects and reduce crystallite sizes which results in increasing edge effects [30]. The G peak is attributed to the first-order scattering of the E_{2g} phonon of sp^2 carbon atoms [31]. The 2D (G′) band originates from the stacking order of nanosheets [32]. The intensity ratio of the D and G bands (I_D/I_G) as a measure of the quality of graphitization or defective disorders on the crystalline graphite is used to determine how modification

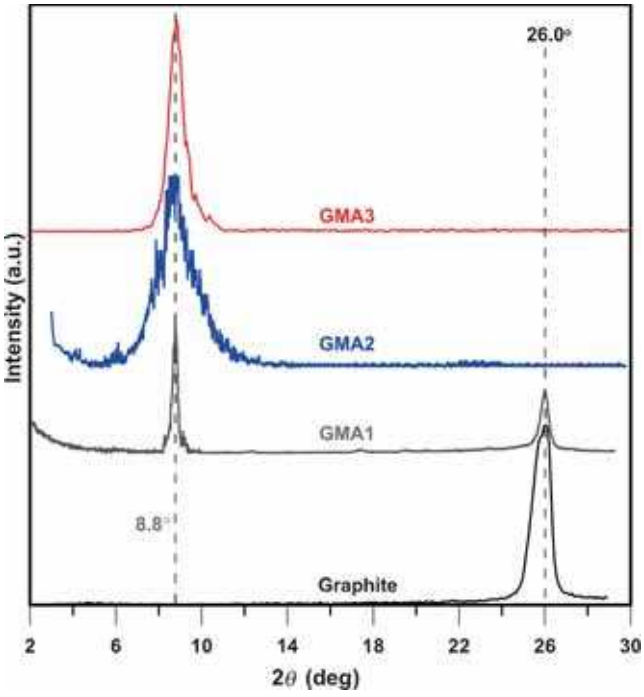

Figure 5. XRD patterns of graphite, GMA1, GMA2 and GMA3.

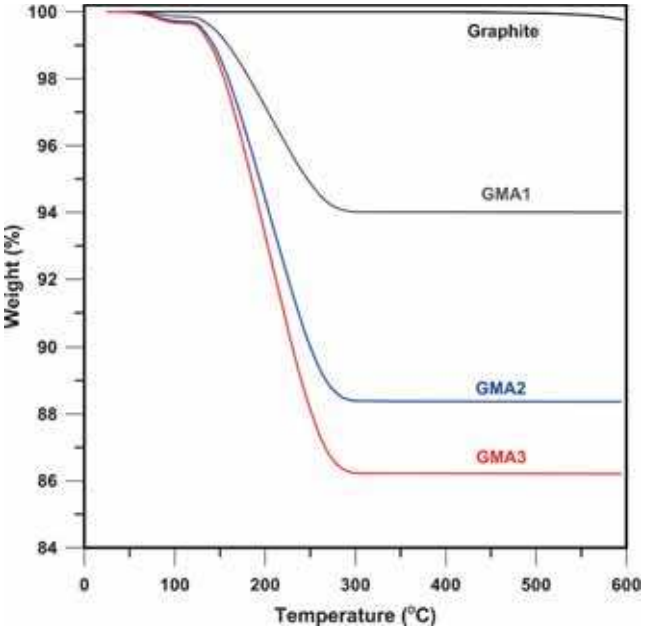

Figure 4. TGA curves of graphite, GMA1, GMA2 and GMA3.

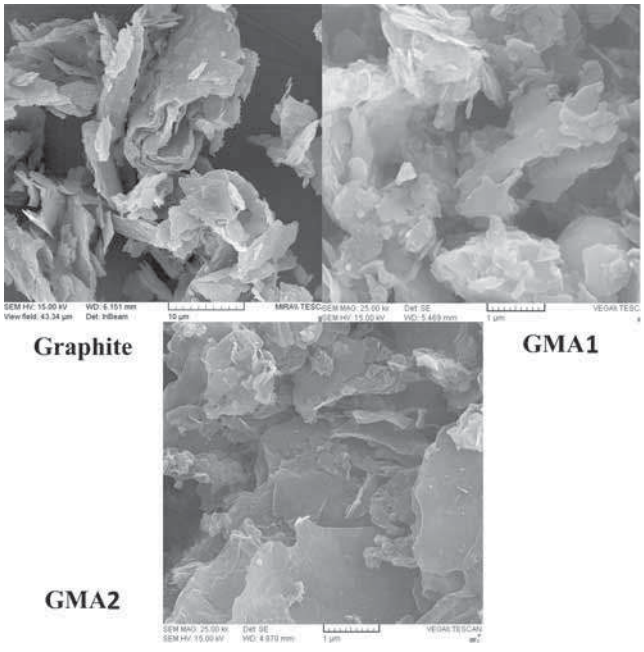

Figure 6. SEM image of graphite, GMA1 and GMA2.

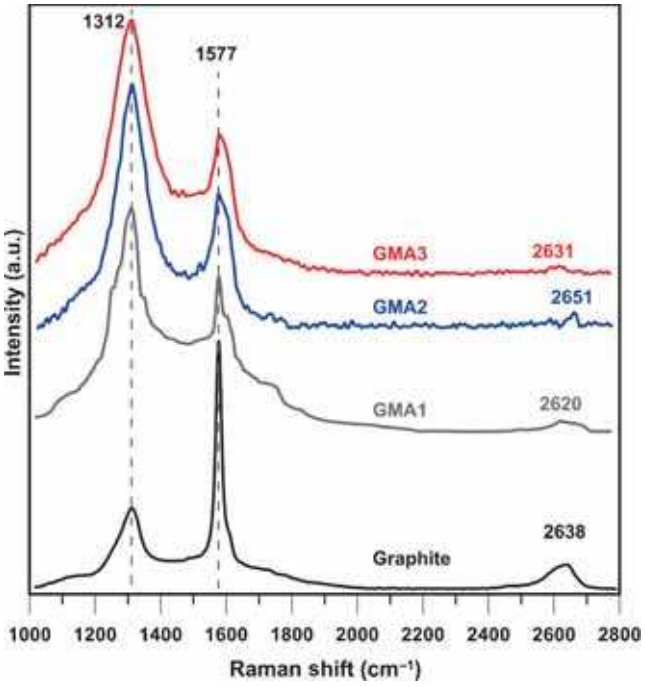

Figure 7. Raman spectra of graphite, GMA1, GMA2 and GMA3.

disrupts the structure of graphite [33]. I_D/I_G value is obtained as 0.32 for graphite that shows low disorder structure. Also, the 2D peak is located at 2639 cm^{-1} with $I_{2D}/I_G = 0.1$. There is no significant shift of peaks' locations in GMA1, GMA2 and GMA3 while the G band becomes broaden with progression of coupling reaction. Broadening of the G band indicate the destruction of sp^2 structure and the formation of defects in the graphene sheets due to graphite's amorphization and modification process [34]. I_D/I_G value increases to 1.14, 1.45 and 1.53 for GMA1, GMA2 and GMA3, respectively, with the predominant D band due to the reduction in size of the in-plane sp^2 domains originated from modification process [35]. Also, the intensity of the 2D peak decreases after modification reaction and the value of I_{2D}/I_G reaches to 0.07, 0.05 and 0.04 for GMA1, GMA2 and GMA3, respectively. Lower value of I_{2D}/I_G shows lower stacking of nanosheets with respect to graphite. I_D/I_G is inversely proportional to the crystallite size (L_a) is depicted as [31]

$$L_a = \left(2.4 \times 10^{-10}\right) \times \lambda_{laser}^4 \left(\frac{I_D}{I_G}\right)^{-1}, \quad (1)$$

where λ_{laser} is the laser excitation wavelength. Therefore, fewer defects result in a higher crystallite size and also a lower I_D/I_G value. It is obvious that after modification process, L_a reduces to 79.4, 62.8 and 59.6 nm for GMA1, GMA2 and GMA3, respectively.

The microstructure of graphite and GMA1 was also studied by means of TEM as depicted in figure 8. TEM study shows graphite as transparent layer where no discernable graphene layers are observed. After modification, surface of nanolayers becomes folded due to the opposite effects of

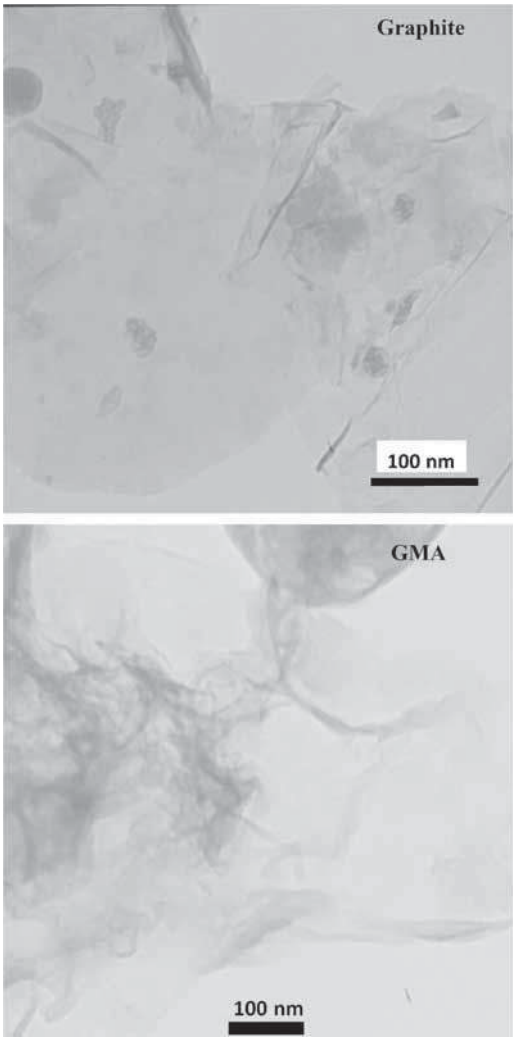

Figure 8. TEM images of graphite and GMA1.

π-conjugated domains and electrostatic repulsion of oxygen-containing groups.

4. Conclusion

Natural graphite was modified via radical coupling using AIBN as radical generator and MAH as modifier with different times of reaction. According to FT-IR and XPS results, it is found that modification process is performed gently where about 6, 11 and 13 wt% of MAH is grafted onto surface of nanosheets after 24, 48 and 72 h, respectively. Although XRD results showed an increase in *d*-spacing of nanolayers, another peak at $2\theta = 26.0°$ showed some graphitic structures as proved by SEM images in early reaction times. However, with increasing reaction time, only a peak related to modified structure remained. According to Raman spectra, I_D/I_G value increased with modification progression and TEM images showed a stacked structure of layers in graphite turned to the folded lamella structure of modified layers.

References

[1] Chen M Q, Quek S S, Sha Z D, Chiu C H, Pei Q X and Zhang Y W 2015 *Carbon* **85** 135

[2] Chang S-L, Wu B-R, Wong J-H and Lin M-F 2014 *Carbon* **77** 1031

[3] Roghani-Mamaqani H, Haddadi-Asl V, Khezri K, Salami-Kalajahi M, Najafi M, Sobani M and Mirshafiei-Langari S-A 2015 *Iran. Polym. J.* **24** 51

[4] Roghani-Mamaqani H, Haddadi-Asl V, Khezri K, Salami-Kalajahi M and Najafi M 2015 *Polym. Eng. Sci.* **55** 1720

[5] Nikdel M, Salami-Kalajahi M and Salami Hosseini M 2014 *Colloid Polym. Sci.* **292** 2599

[6] Samadaei F, Salami-Kalajahi M, Roghani-Mamaqani H and Banaei M 2015 *RSC Adv.* **5** 71835

[7] Shaffer M S P and Koziol K 2002 *Chem. Commun.* 2074

[8] Razavi Aghjeh M K, Nazockdast H and Assempour H 2006 *J. Appl. Polym. Sci.* **99** 141

[9] Sheshkali H R Z, Assempour H and Nazockdast H 2007 *J. Appl. Polym. Sci.* **105** 1869

[10] Chen Z, Fang P, Wang H and Wang S 2008 *J. Appl. Polym. Sci.* **107** 985

[11] Liu X, Hu Y, Liang M, Li Y, Yin J and Yang W 2004 *Fluid Phase Equilibria* **367** 1

[12] Wang T and Shen Y 2011 *Adv. Mater. Res.* **233–235** 1623

[13] Amirshaqaqi N, Salami-Kalajahi M and Mahdavian M 2014 *Iran. Polym. J.* **23** 699

[14] Salami-Kalajahi M, Haddadi-Asl V, Behboodi-Sadabad F, Rahimi-Razin S and Roghani-Mamaqani H 2012 *Polym. Compos.* **33** 215

[15] Barra G M O, Crespo J S, Bertolino J R, Soldi V and Pires A T N 1999 *J. Braz. Chem. Soc.* **10** 31

[16] Yang L, Zhang F, Endo T and Hirotsu T 2003 *Macromolecules* **36** 4709

[17] de los Santos E G, Gonzalez M J L and Gonzalez M C 1998 *J. Appl. Polym. Sci.* **68** 45

[18] Torkpur-Biglarianzadeh M and Salami-Kalajahi M 2015 *RSC Adv.* **5** 29653

[19] Amirshaqaqi N, Salami-Kalajahi M and Mahdavian M 2014 *Corros. Sci.* **87** 392

[20] Nakajima T, Žemva B and Tressaud A 2000 *Advanced inorganic fluorides: synthesis, characterization and applications* (Elsevier) p 511

[21] Wen Y, He K, Zhu Y, Han F, Xu Y, Matsuda I, Ishii Y, Cumings J and Wang C 2014 *Nat. Commun.* **5** Article number: 4033

[22] Chen J, Li Y, Huang L, Li C and Shi G 2015 *Carbon* **81** 826

[23] Roghani-Mamaqani H, Haddadi-Asl V, Khezri K and Salami-Kalajahi M 2014 *Polym. Int.* **63** 1912

[24] Mishra G and McArthur S L 2010 *Langmuir* **26** 9645

[25] Sun Z, Nicolosi V, Rickard D, Bergin S D, Aherne D and Coleman J N 2008 *J. Phys. Chem. C* **112** 20264

[26] Liu J, Scott C, Winroth S, Maia J and Ishida H 2015 *RSC Adv.* **5** 16785

[27] Salami-Kalajahi M, Haddadi-Asl V, Behboodi-Sadabad F, Rahimi-Razin S, Roghani-Mamaqani H and Hemmati M 2012 *Nano* **7** 1250003

[28] Nikdel M, Salami-Kalajahi M and Salami Hosseini M 2014 *RSC Adv.* **4** 16743

[29] Rahimi-Razin S, Salami-Kalajahi M, Haddadi-Asl V and Roghani-Mamaqani H 2012 *J. Polym. Res.* **19** 9954

[30] Fang M, Wang K, Lu H, Yang Y and Nutt S 2010 *J. Mater. Chem.* **20** 1982

[31] Roghani-Mamaqani H, Haddadi-Asl V, Khezri K, Zeinali E and Salami-Kalajahi M 2014 *J. Polym. Res.* **21** Article no. 333

[32] Roghani-Mamaqani H, Haddadi-Asl V, Khezri K and Salami-Kalajahi M 2014 *RSC Adv.* **4** 24439

[33] Rahimi-Razin S, Haddadi-Asl V, Salami-Kalajahi M, Behboodi-Sadabad F and Roghani-Mamaqani H 2012 *J. Iran. Chem. Soc.* **9** 877

[34] Kudin K N, Ozbas B, Schniepp H C, Prud'homme R K, Aksay I A and Car R 2008 *Nano Lett.* **8** 36

[35] Stankovich S, Dikin D A, Piner R D, Kohlhaas K A, Kleinhammes A, Jia Y, Wu Y, Nguyen S T and Ruoff R S 2007 *Carbon* **45** 1558